

## Full-length article

## Inhibitory effects of coronary vasodilator papaverine on heterologously-expressed HERG currents in *Xenopus* oocytes

Cuk-seong KIM<sup>1</sup>, Nam LEE<sup>1</sup>, Sook-jin SON<sup>1</sup>, Kyu-seung LEE<sup>1</sup>, Hyo-shin KIM<sup>1</sup>, Yong-geun KWAK<sup>2</sup>, Soo-wan CHAE<sup>2</sup>, Sang-do LEE<sup>1</sup>, Byeong-hwa JEON<sup>1</sup>, Jin-bong PARK<sup>1,3</sup>

<sup>1</sup>Department of Physiology, College of Medicine, Chungnam National University, Daejeon 301131, Korea; <sup>2</sup>Department of Pharmacology, Chonbuk National University, Medical School, Chonju 561-180, Korea

### Key words

papaverine; HERG; cardiac action potential

<sup>3</sup> Correspondence to Dr Jin-bong PARK.

Phn 82-42-580-8212.

Fax 82-42-545-8440.

E-mail jinbong@cnu.ac.kr

Received 2006-08-30

Accepted 2006-10-10

doi: 10.1111/j.1745-7254.2007.00507.x

### Abstract

**Aim:** To characterize the effects of papaverine on HERG channels expressed in *Xenopus* oocytes as well as cardiac action potential in rabbit ventricular myocytes. **Methods:** Conventional microelectrodes were used to record action potential in rabbit ventricular myocytes. HERG currents were recorded by 2-electrode voltage clamp technique in *Xenopus* oocytes injected with HERG cRNA. **Results:** Papaverine increased the cardiac action potential duration in rabbit ventricular myocytes. It blocked heterologously-expressed HERG currents in a concentration-dependent manner ( $IC_{50}$  71.03±4.75 µmol/L,  $NH$  0.80,  $n=6$ ), whereas another phosphodiesterase inhibitor, theophylline (500 µmol/L), did not. The blockade of papaverine on HERG currents was not voltage-dependent. The slope conductance measured as a slope of the fully activated HERG current-voltage curves decreased from 78.03±4.25 µS of the control to 56.84±5.33, 36.06±6.53, and 27.09±5.50 µS ( $n=4$ ) by 30, 100, and 300 µmol/L of papaverine, respectively. Papaverine (100 µmol/L) caused a 9 mV hyperpolarizing shift in the voltage-dependence of steady-state inactivation, but there were no changes in the voltage-dependence of HERG current activation. Papaverine blocked HERG channels in the closed, open, and inactivated states. **Conclusion:** These results showed that papaverine blocked HERG channels in a voltage- and state-independent manner, which may most likely be the major mechanism of papaverine-induced cardiac arrhythmia reported in humans.

### Introduction

Papaverine (6,7-dimethoxy-1-veratrylisoquinoline), a substituted alkaloid from *Papaver somniferum*, has been known to relax many kinds of smooth muscles. Because of its relaxant effects on smooth muscle, papaverine has been used as a vasodilator agent<sup>[1–3]</sup> and a therapeutic agent for renal colic<sup>[4]</sup> and penile impotence<sup>[5]</sup>. It was also proposed as an “ideal coronary vasodilator”<sup>[1]</sup>. Additionally, intra-arterial papaverine infusion has been used for the prevention and treatment of vasospasm following subarachnoid hemorrhage<sup>[6,7]</sup>. However, under certain clinical settings, such as cases of overdose, papaverine induced cardiac arrhythmias including prolonged QT intervals that can lead to the life-threatening

ventricular arrhythmia, torsades de points<sup>[8–11]</sup>.

One means by which drugs can prolong QT intervals is through the inhibition of one or more repolarizing  $K^+$  channel currents in the myocardium<sup>[12,13]</sup>. In humans, the most common channel linked to drug-induced QT interval prolongation is the rapid component of the delayed rectifier  $K^+$  channel ( $I_{Kr}$ )<sup>[14]</sup>. The human ether-a-go-go-related gene, HERG, encodes the pore-forming subunit of  $I_{Kr}$ <sup>[15,16]</sup>. Naturally, many drugs associated with QT interval prolongation have been found to block HERG channels<sup>[17–21]</sup>. It can be assumed therefore that papaverine may cause LQT by inhibiting HERG/ $I_{Kr}$ . To examine this possibility, we investigated the effect of papaverine on HERG currents expressed in *Xenopus* oocytes. We found that papaverine

effectively inhibited HERG currents in a state-independent manner in *Xenopus* oocytes.

## Materials and methods

**Recording of the action potential in rabbit cardiac myocytes** Rabbits (Male, New Zealand white rabbits, weighing 1.8–2.0 kg each) were anesthetized by injections of thiopental sodium (10 mg/kg) into a marginal ear vein. Their hearts were rapidly excised and transferred to Tyrode's solution (137 mmol/L NaCl, 5.4 mmol/L KCl, 1.05 mmol/L MgCl<sub>2</sub>, 1.8 mmol/L CaCl<sub>2</sub>, 5 mmol/L glucose, and 10 mmol/L HEPES at pH 7.4), and the hearts were oxygenated with 100% O<sub>2</sub> at room temperature. The ventricular muscles (1.5–2 mm in width and 2–4 mm in length) were carefully dissected from the left ventricular wall. All tissues were less than 1 mm in depth.

Each specimen of the dissected tissue was mounted horizontally in a recording chamber, and continuously superfused with oxygenated Tyrode's solution at a rate of 5 mL/min. One end of each tissue was fixed by an insect pin to the bottom of the chamber coated with Sylgard. The tissue next to the insect pin was pressed against the chamber floor by stimulation electrodes, which were used to elicit the action potentials. The cardiac tissues were stimulated with square pulses (2 Hz, 1 ms duration, 20%–30% above the threshold voltage) using a stimulator with a stimulus isolation unit (WPI, Sarasota, FL, USA). After allowing 2 h for stabilization, the action potentials were recorded with a 3 mol/L KCl-filled conventional microelectrode (20–30 MΩ) that was connected to an amplifier (KS-700, WPI, USA), and these action potentials were displayed on an oscilloscope (Dual beam storage 5113, Tektronix, Beaverton, OR, USA). After 1 h of stabilization of recording, the drugs were applied.

**Oocyte preparation** Oocytes were prepared as described previously<sup>[22]</sup>. Briefly, ovarian lobes excised from the anesthetized *Xenopus laevis* (*Xenopus* I, USA) were treated with 0.2% collagenase (type II, Sigma Co, St Louis, MO, USA) for 1–2 h in Ca<sup>2+</sup>-free Barth's solution. The composition of Ca<sup>2+</sup>-free Barth's solution is as follows: 88.7 mmol/L NaCl, 1.0 mmol/L KCl, 2.4 mmol/L NaHCO<sub>3</sub>, 0.8 mmol/L MgSO<sub>4</sub>·7H<sub>2</sub>O, and 5 mmol/L HEPES (pH=7.5). cRNA (50 nL, 0.3–1.0 ng/nL) of HERG synthesized from the linearized cDNA using *in vitro* transcription kit (Ambion Inc, Austin, TX, USA) was injected in stage V or VI oocytes with glass capillaries connected with a microdispenser (VWR Scientific Co, Grove, IL, USA). After the injection, oocytes were cultured at 18 °C in Barth's solution containing 88.0 mmol/L NaCl, 1.0 mmol/L KCl, 2.4 mmol/L NaHCO<sub>3</sub>, 0.8 mmol/L MgSO<sub>4</sub>·7H<sub>2</sub>O, 0.3 mmol/L Ca(NO<sub>3</sub>)<sub>2</sub>·4H<sub>2</sub>O, 0.4 mmol/L CaCl<sub>2</sub>, and 5 mmol/L HEPES (pH=

7.5), supplemented with 2 mmol/L pyruvate and 50 g/mL gentamicin sulfate. The culture medium was changed daily. Currents were recorded from 2 to 7 d after injection.

**Whole cell current recording in *Xenopus* oocytes** HERG currents were recorded using a 2-electrode voltage-clamp amplifier (OC-725C, Warner Instruments, Hamden, CT, USA) from the oocytes placed in the recording chamber (2.0 mL) superfused with Oocyte-Ringer solution containing 96.0 mmol/L NaCl, 2.0 mmol/L KCl, 1.0 mmol/L MgCl<sub>2</sub>, 1.8 mmol/L CaCl<sub>2</sub>·2H<sub>2</sub>O, and 5.0 mmol/L HEPES (pH=7.5). Stimulation and data acquisition were controlled with Digidata 1200 (Axon Instruments) and pClamp 6.04 (Axon Instruments, USA). Electrodes were fabricated from glass capillaries containing an inner filament (OD 1.5 mm, ID 1.12 mm; WPI, USA). Electrodes filled with 3 mol/L KCl had a resistance of 1–2 for current-passing electrodes and 2–4 for voltage-recording electrodes.

**Data analysis** The voltage dependence of HERG current activation was determined for each oocyte by fitting peak values of the tail current ( $I_{tail}$ ) versus test potential ( $V_t$ ) to a Boltzmann function:

$$I_{tail} = \frac{I_{tail}^{max}}{1 + \exp\left(\frac{V_{1/2} - V_t}{k}\right)}$$

Where  $I_{tail}^{max}$  is the maximum tail current,  $V_{1/2}$  is the voltage at which 50% of the channels are activated, and  $k$  is the slope factor. To examine steady-state inactivation, conditioning pulses between -130 and +20 mV in 10 mV increments for 60 ms were applied after a depolarizing pulse to +20 mV for 900 ms, followed by a common test pulse to +20 mV. The peak current amplitudes during the test pulses were plotted as a function of the previous conditioning pulses. Normalized steady-state inactivation as a function of prepulse of test potential was also fitted to a Boltzmann function. The data were expressed as the mean±SEM. Paired Student's *t*-test was used to compare the drug effect on HERG currents. ANOVA repeated measures, followed by Tukey's *post-hoc* tests were used to study concentration-dependent drug effects.

**Drugs** All drugs were purchased from Sigma Co (St Louis, USA). Papaverine was dissolved in 10–3 mol/L stock solution and stored at 4 °C until dilution within the perfusion solution immediately before use.

## Results

To identify the general electrophysiological effect of papaverine on cardiac action potential, we examined the effects of papaverine on cardiac action potential in isolated

rabbit ventricular myocytes stimulated at a frequency of 2 Hz (Figure 1). After 20 min of exposure, the action potential duration at 90% repolarization (APD<sub>90</sub>) in the ventricular myocytes increased from 219±5 ms to 267±6 ms and 355±18 ms (n=4) by 10 and 30 μmol/L papaverine, respectively. Resting membrane potential was depolarized from -81±3 mV to -77±4 mV (n=3) by 30 μmol/L papaverine, but not by 10 μmol/L papaverine (-81±5 mV, n=4).

The effect of papaverine on HERG currents was studied in *Xenopus* oocytes injected with HERG mRNA. Figure 2A shows voltage-clamp data obtained 10 min after application of 100 μmol/L of papaverine. Families of current traces from 1 cell are shown for control conditions and after exposure to papaverine with the voltage protocol shown in Figure 2A. Cells were clamped at a holding potential of -80 mV. Depolarizing steps were applied for 4 s to voltages between -70 and +40 mV in 10 mV increments. Papaverine (100 μmol/L) suppressed both the outward and tail currents (Figure 2A),

which was only partially (72%±8% of the control, n=4) recovered in the 30 min drug wash-out. Current-voltage plots of outward currents present at the end of the depolarizing step and peak tail current are depicted in Figure 2B and 2C, respectively. Current amplitudes were normalized to peak values obtained from each cell. For control conditions, the threshold for activating HERG currents was close to -40 mV, and full activation was obtained at a voltage close to +10 mV. In the presence of 100 μmol/L of papaverine, outward currents at the depolarizing step and tail current amplitude were reduced, compared with control condition, to ~40% at all tested potentials.

**Papaverine blocked HERG currents in a concentration-dependent manner** Steady-state block was obtained by applying depolarizing steps from -80 to 0 mV for the 10 s period every 30 s, and peak tail current was measured after the repolarizing steps to -40 mV for 6 s at different drug concentrations. Analysis of the data with the Hill equation

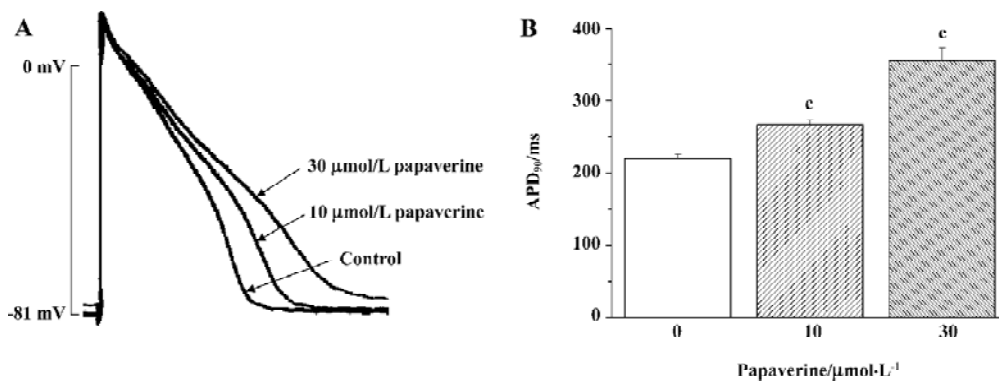


**Figure 1.** Effects of papaverine on the APD<sub>90</sub> of rabbit ventricular myocytes. (A) Representative traces show papaverine prolonged the APD of rabbit ventricular myocytes. (B) Averaged values of APD<sub>90</sub> in the presence of 10 μmol/L and 30 μmol/L of papaverine, respectively, were compared with the control values. Each column with a vertical bar represents mean SEM (n=4). \*P<0.01.

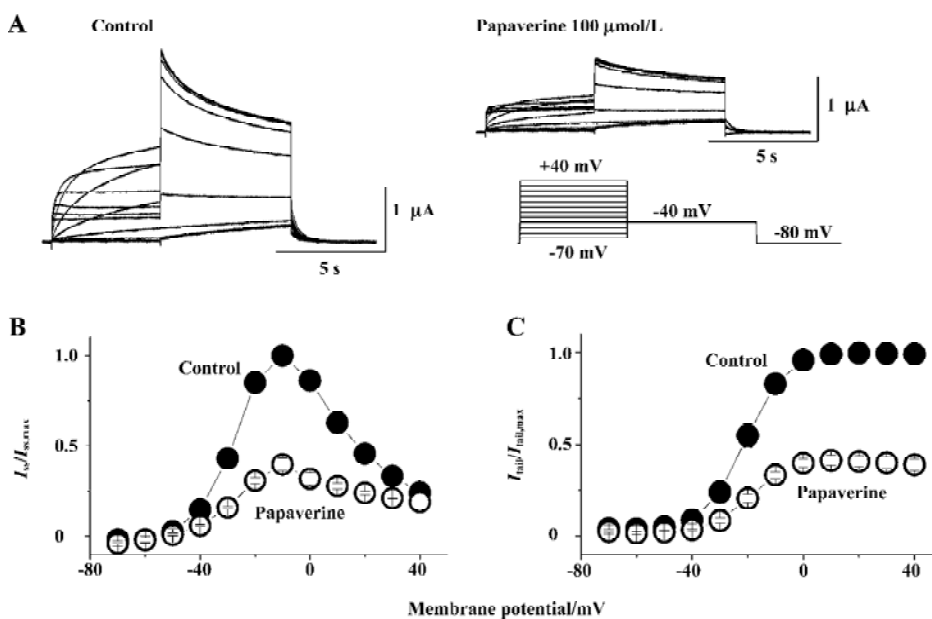


**Figure 2.** Effect of papaverine on HERG current expressed in *Xenopus* oocytes. (A) Traces of HERG currents were recorded before and after exposure to 100 μmol/L of papaverine for 10 min using voltage protocol shown as inset. Current-voltage plots of steady-state (B) and peak tail currents (C) in the absence or presence of 100 μmol/L of papaverine. Currents were normalized to the maximum steady-state (B) or peak tail currents (C) in the absence of papaverine in each oocyte. Each point with vertical bar denotes the mean SEM (n=6).

gave a half-maximal inhibitory concentration ( $IC_{50}$ ) value of  $71.0 \mu\text{mol/L}$  and Hill coefficient of 0.81 (Figure 3).

Papaverine is known as a phosphodiesterase inhibitor. To determine whether the effect of papaverine on HERG was related to phosphodiesterase inhibition, the effects of theophylline, another phosphodiesterase inhibitor, on HERG currents was investigated. Theophylline ( $500 \mu\text{mol/L}$ ) did not affect HERG currents (Figure 4A), which were completely blocked by dofetilide (Figure 4B), known to be a selective  $I_{Kr}$  blocker, suggesting that the papaverine block on HERG is independent from the phosphodiesterase inhibition.

Drugs that block ion channels often alter the voltage dependence of channel kinetics. Therefore, we also analyzed the voltage dependence of the activation of the peak amplitude of the decaying tail currents in the absence or presence of papaverine ( $100 \mu\text{mol/L}$ ). The voltage depen-

dence of the HERG activation was determined using 4 s test pulses to potentials ranging from  $-70$  to  $+40$  mV. Peak amplitudes of tail currents were measured at  $-40$  mV, plotted as a function of test potential, and were fitted with a Boltzmann function (Figure 2C). In the control experiment, the activation curve had a midpoint of  $-16.4 \pm 1.1$  mV and a slope factor of  $6.8 \pm 0.4$  mV ( $n=6$ ). There was no significant change in voltage dependence of the activation curve ( $V_{1/2} -16.5 \pm 2.4$  mV and a slope factor of  $5.8 \pm 1.5$  mV,  $n=6$ ,  $P>0.05$  vs the control in both) by papaverine.

We also investigated the effects of papaverine at a concentration of  $100 \mu\text{mol/L}$  on the inactivation of HERG currents. Steady-state inactivation currents were studied before and after the application of papaverine using a dual-pulse protocol as described in Materials and methods. The steady-state inactivation curve was shifted to a negative potential

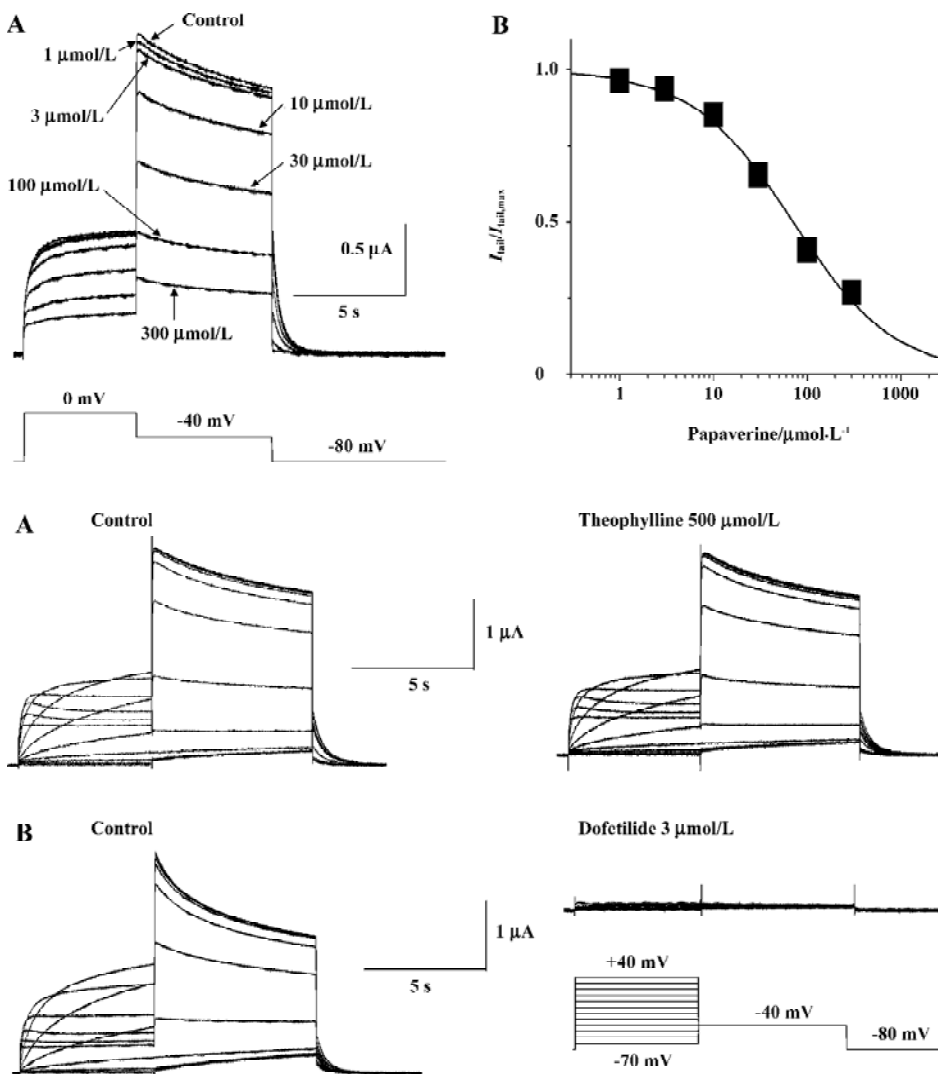


**Figure 3.** Concentration dependence of papaverine block on HERG current. (A) representative current traces from an oocyte depolarized to 0 from a holding potential of  $-80$  mV, in the presence of various concentrations of papaverine. Tail currents were recorded at  $-40$  mV. (B) amplitudes of peak tail currents were normalized to the maximum current obtained in the control, and plotted against papaverine concentrations. Data were fitted with a Hill equation. Each point with vertical bars represents mean  $\pm$  SEM ( $n=6$ ). All error bars are in the range of symbols.

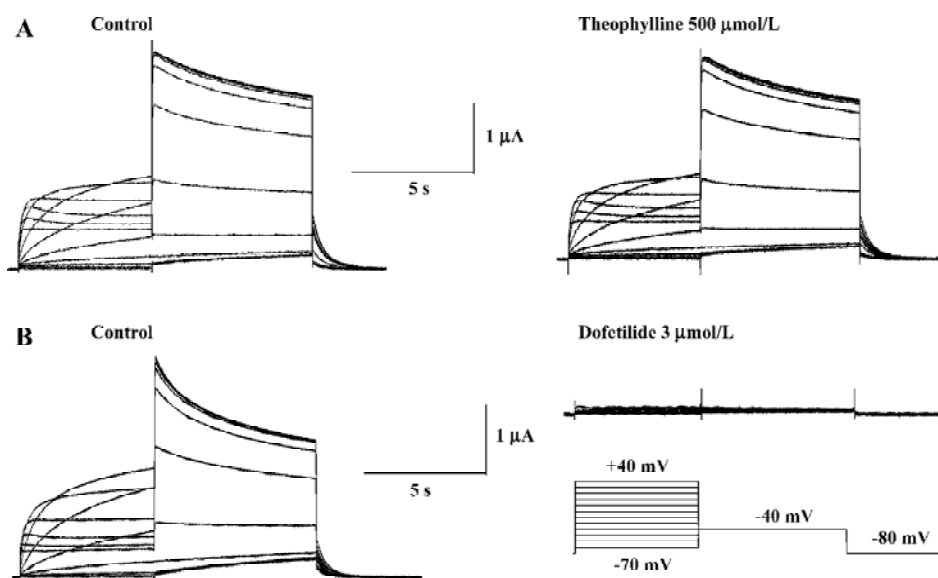


**Figure 4.** Effect of theophylline and dofetilide on HERG current expressed in *Xenopus* oocytes. Representative traces of HERG currents were recorded before and after exposure to  $500 \mu\text{mol/L}$  theophylline (A) and  $3 \mu\text{mol/L}$  dofetilide (B). Voltage protocols were the same as those described in Figure 1. Similar results were observed from 4 oocytes for each drug.

( $V_{1/2}$   $-68.7 \pm 3.2$  mV in the control and  $-77.4 \pm 1.6$  mV after papaverine,  $P < 0.05$ ,  $n = 5$ ; Figure 5). The slope factor of steady-state inactivation decreased slightly from  $24.3 \pm 2.9$  mV in the control to  $17.2 - 1.3$  mV in the presence of papaverine.

To directly test the effect of papaverine on HERG inactivation, we examined the time course of inactivation in the absence and presence of papaverine. The inactivation time course of expressed currents was analyzed by applying brief hyperpolarizing pulses to allow the HERG channel to recover from inactivation after an initial long depolarizing pulse. Depolarizing test pulses were then applied to record inactivating currents (Figure 5C). The time course of fast, inactivating currents could be fitted by a single-exponential function. In the presence of papaverine, the time constants for inactivation significantly decreased at all tested potentials (Figure 5D). Recovery from inactivation was also measured using the same pulse protocol shown in Figure 4. Tail currents could be fitted by a double-exponential function,

and the fast component was defined as the time constant of recovery from inactivation. In the presence of papaverine, the time constants for inactivation and recovery from inactivation significantly decreased at all potentials (Figure 5D).

To further delineate the underlying mechanism for papaverine inhibition of HERG currents, we examined the fully activated  $I-V$  relationships by applying various test potentials after a depolarizing conditioning pulse (Figure 6). The slope conductance measured as a slope of the current-voltage relationship curve between  $-130$  and  $-110$  mV decreased from  $78.03 \pm 4.25$   $\mu$ S of the control to  $56.84 \pm 5.33$ ,  $36.06 \pm 6.53$ , and  $27.09 \pm 5.50$   $\mu$ S ( $n = 6$ ) in the presence of 30, 100, and 300  $\mu$ mol/L papaverine, respectively ( $P < 0.05$  vs the control at each concentration).

On the basis of single-channel studies, a 5-state model has been suggested for HERG channels summarizing 1 open, 1 inactivated, and 3 closed states<sup>[23]</sup>. Therefore, we investigated whether papaverine block is state dependent (Figure 7). After the control currents were measured, the membrane

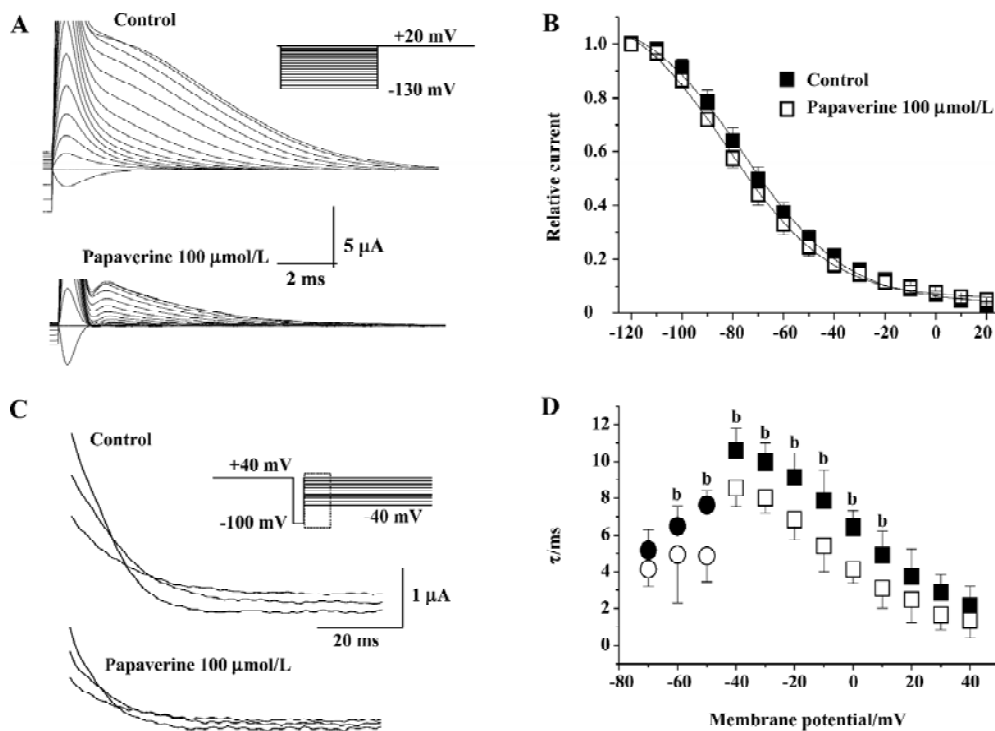


**Figure 5.** Effect of papaverine on HERG inactivation. (A) representative current traces for steady-state inactivation using a double-pulse protocol with conditioning pulses between  $-130$  mV and  $+20$  mV (upper inset). (B) mean normalized steady-state inactivation curves for the control and after  $100$   $\mu$ mol/L papaverine were fitted with a Boltzmann function. Each point with a vertical bar denotes the mean  $\pm$  SEM ( $n = 6$ ). (C) Representative current traces for HERG current onset of inactivation by using the protocol shown upper inset. Region of interest is magnified only at  $-40$  mV,  $-20$ , and  $0$  mV for clarity. (D) time constants for onset of inactivation are plotted against the membrane potential (between  $-40$  mV and  $+40$  mV). With the same voltage protocol in Figure 4, recovery from inactivation was measured by fitting a double exponential function to the rising phase of tail current trace at each potential (between  $-70$  mV and  $-50$  mV). Data are expressed as mean  $\pm$  SEM ( $n = 6$ , <sup>b</sup> $P < 0.05$ , control vs  $100$   $\mu$ mol/L papaverine).

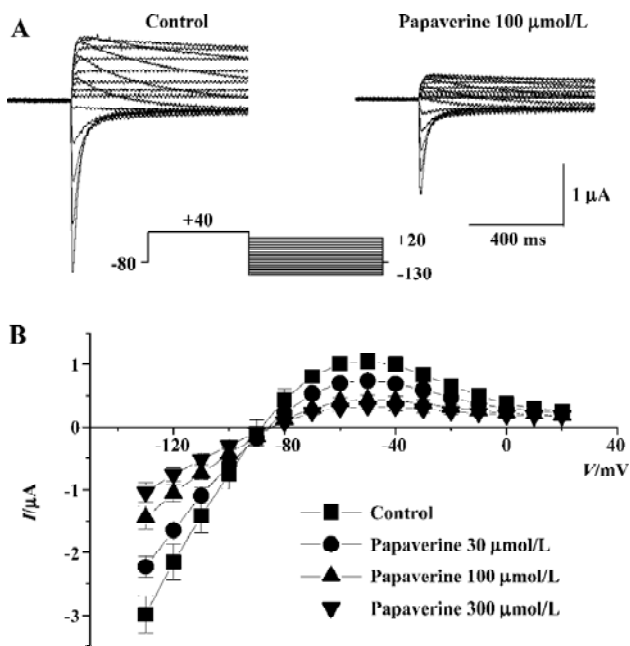


**Figure 6.** Effect of papaverine on HERG conductance. (A) representative current traces with a conditioning pulse to +40 mV for 750 ms from a holding potential of -80 mV, followed by test pulse to various potentials between -130 mV and +20 mV in 10 mV increments (inset). (B) current-voltage plots of maximum currents in the absence or presence of papaverine (30–300  $\mu\text{mol/L}$ ). Each point with a vertical bar denotes the mean $\pm$ SEM ( $n=6$ ).

potential was held at -80 mV to keep the channel in the closed conformation during wash-in of 100  $\mu\text{mol/L}$  of papaverine. The first depolarization to 0 mV after 10 min at -80 mV yielded most of the blocking effect. The initial current inhibition ( $61.0\% \pm 4.6\%$ ,  $n=4$ ) reflects that papaverine bound HERG without channel opening and/or activation, whereas the additional time-dependent inhibition ( $4.8\% \pm 2.2\%$ ,  $n=4$ ) observed after channel activation may represent additional papaverine inhibition on HERG channels during the open state.

## Discussion

In the present study, we show that a clinical vasodilator, papaverine, increases cardiac action potential duration and inhibits cardiac  $\text{K}^+$  channel HERG expressed in *Xenopus* oocytes. Papaverine has been shown to prolong QT intervals and cause ventricular arrhythmia<sup>[11]</sup>. Many commonly used drugs, including antiarrhythmic, antihistamine, antipsychotic, and antibiotic agents are associated with drug-induced LQTS. Most of these drugs either block HERG-dependent  $\text{K}$  current ( $I_{\text{Kr}}$ ) in ventricular myocytes or inhibit liver enzymes that are important for metabolic degradation of other drugs that block  $I_{\text{Kr}}$ . It is well known that heterolo-

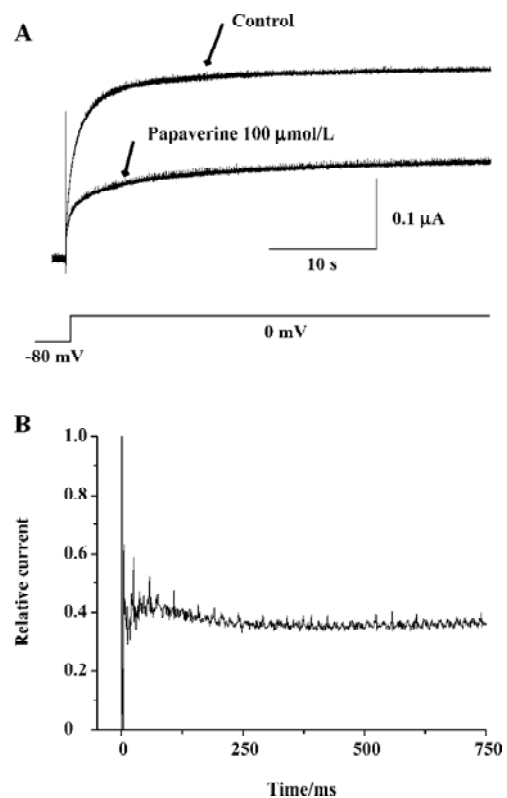


**Figure 7.** State dependence of HERG block by papaverine. (A) HERG currents were activated by a 20 s depolarizing voltage step to 0 mV from a holding potential of -80 mV. After the control measurement, the oocyte was held at -80 mV for 15 min during perfusion with 100  $\mu\text{mol/L}$  papaverine. The control recording and the first pulse measured immediately after the incubation period are displayed. (B) Relative current representing the residual current ratio compared to the control in the presence of 100  $\mu\text{mol/L}$  of papaverine for the first 2 s. The relative current was not estimated to start at 0 with the activation of the channel. Note the additional relative current decrease from 40% to 33% in 300 ms after channel activation.

gously-expressed HERG currents share pharmacological and biophysical properties with  $I_{\text{Kr}}$ <sup>[15,16]</sup>. The characteristics of the currents recorded in the present study correspond to HERG currents: slow current activation at negative potentials, large long-lasting tail currents on repolarization, strong inward rectification, and sensitivity to class III antiarrhythmic methanesulfonanilide such as dofetilide (Figure 4). Considering all of these, papaverine may cause LQT through the inhibition of HERG/ $I_{\text{Kr}}$  in cardiac myocytes. The present study is the first to characterize the interaction between papaverine and HERG showing an ionic mechanism underlying papaverine-induced ventricular arrhythmia.

The major finding of the present study is that papaverine blocks HERG channels in a concentration-dependent, but voltage- and state-independent manner in *Xenopus* oocytes.

Taken into account that *in vitro* data is influenced by several artificial factors such as expression system properties, temperature, and lack of subunits, the degree of HERG blocked by papaverine seems appropriate. The affinity of ion channel blockers is reduced in *Xenopus* oocytes due to follicular tissues and the yolk<sup>[24]</sup>. Consistent with this, papaverine inhibited HERG currents with an IC<sub>50</sub> of ~70 μmol/L in *Xenopus* oocytes (Figure 3), and significantly increased action potential duration in rabbit myocytes at 10 μmol/L of papaverine (Figure 1). This suggests the different pharmacokinetics of papaverine in the 2 different cells. However, we cannot exclude the possibility that papaverine may affect other ionic currents<sup>[25,26]</sup> in addition to the blockage of I<sub>Kr</sub>, for it depolarized resting membrane potential in ventricular myocytes. Further evaluation of IC<sub>50</sub> of papaverine on I<sub>Kr</sub> in ventricular myocytes will be helpful to address it.

The state-dependence of HERG channel block has been described for numerous substances, such as bertosamil<sup>[27]</sup>, fluvoxamine<sup>[28]</sup>, and KCB-328<sup>[29]</sup> with the majority of those binding to the channel in the open state. Choe *et al*<sup>[25]</sup> provide evidence for open channel blockade by papaverine in their studies of Kv1.5 stably expressed in Ltk- cells by demonstrating the accelerated decline of the current during depolarization, as well as steeper blockade in the voltage range of the channel opening. The Kv1.5 current is a rapidly activating and relatively slow inactivating delayed rectifier current, and this differs significantly from the HERG channel. In the present study, papaverine did not modify the time course of channel activation. If present, a tail current “crossover”, due to transient channel unblocking during repolarization<sup>[30]</sup>, provides evidence for open channel block. This was not seen in the present study. Depolarization of membrane potential did not increase HERG current inhibition by papaverine at which most channels would be in the inactivated state. Consistent with the tonic block achieved without channel opening or activation (Figure 7), these results suggest that papaverine mainly bind closed HERG channels.

Various drugs inhibit HERG currents binding to the inactivated HERG channel<sup>[32]</sup>. Sites in the outer pore region such as G628, G631, S620, A614, and V630 have been known to involve HERG channel inactivation, which also postulated as a binding site(s) of the drug acting with the inactivated HERG channel<sup>[33]</sup>. H587 of the S5-P loop<sup>[34]</sup> and M651 of the S6 sites<sup>[35]</sup> also involved HERG inactivation kinetics. Papaverine markedly accelerated inactivation at most potentials, consistent with the observed 9 mV hyperpolarizing shift in the voltage-dependence of HERG channel inactivation, which implies a decrease in channel availability<sup>[31]</sup>. Papaverine also

markedly increased the rate of recovery from inactivation (Figure 5D). These data imply that the drug acts on inactivated HERG. Therefore, we may speculate that these sites involved in HERG inactivation at least partly contribute to HERG inhibition by papaverine.

There is no consensus about confirming the threshold for the predication of clinically important HERG channel blockade based on an *in vitro* model. One hypotheses is that drugs will be free of liability for the ventricular arrhythmia torsades de pointes if they fail to produce a 20% blockade at the highest achievable free plasma concentration<sup>[36]</sup>. Another hypothesis is that drugs for which the IC<sub>50</sub> is at least 30-fold greater than the highest achievable free or total plasma concentration will be free of liability for torsades de pointes<sup>[18,36]</sup>. Although limited data are available with regard to expected maximum plasma concentrations after administration of papaverine, it reached to 49.4–56.6 μmol/L with various carriers in rabbits<sup>[37]</sup>. The values are similar to papaverine IC<sub>50</sub> on HERG block even in *Xenopus* oocytes. Although maximum C<sub>max</sub> values would be useful in estimating a worst-case clinical relevance of HERG channel blockade, it is notable that papaverine did cause arrhythmia in humans<sup>[8–11]</sup>.

In summary, this report is the first to detail the effects of papaverine on HERG, explaining cellular mechanism for QT prolongation. We found that papaverine blocked HERG currents via binding closed, open, and inactivated channels. These blocking properties may contribute to the arrhythmogenic properties of papaverine.

## References

- 1 Wilson RF, White CW. Intracoronary papaverine: an ideal coronary vasodilator for studies of the coronary circulation in conscious humans. *Circulation* 1986; 73: 444–51.
- 2 Franz N, Modersohn D, Romaniuk P, Linss G. Coronary reserve determination by intracoronary papaverine: effects of various doses on coronary circulation and hemodynamics. *Z Gesamte Inn Med* 1991; 46: 15–7.
- 3 Newell DW, Elliott JP, Eskridge JM, Winn HR. Endovascular therapy for aneurysmal vasospasm. *Crit Care Clin* 1999; 15: 685–99.
- 4 Jonsson PE, Olsson AM, Petersson BA, Johansson K. Intravenous indomethacin and oxycone-papaverine in the treatment of acute renal colic. A double-blind study. *Br J Urol* 1987; 59: 396–400.
- 5 Handelsman H. Diagnosis and treatment of impotence. *Health Technol Assess Rep* 1990; 2: 1–23.
- 6 Flemming KD, Brown RD Jr, Wiebers DO. Subarachnoid hemorrhage. *Curr Treat Options Neurol* 1999; 1: 97–112.
- 7 Tsurushima H, Hyodo A, Yoshii Y. Papaverine and vasospasm. *J Neurosurg* 2000; 92: 509–11.
- 8 Jain A, Jenkins MG. Intracoronary electrocardiogram during *torsade des pointes* secondary to intracoronary papaverine.

- Cathet Cardiovasc Diagn 1989; 18: 255–7.
- 9 Kern MJ, Deligonul U, Serota H, Gudipati C, Buckingham T. Ventricular arrhythmia due to intracoronary papaverine: analysis of QT intervals and coronary vasodilatory reserve. *Cathet Cardiovasc Diagn* 1990; 19: 229–36.
  - 10 Vrolix M, Piessens J, De Geest H. *Torsades de pointes* after intracoronary papaverine. *Eur Heart J* 1991; 12: 273–6.
  - 11 Inoue T, Asahi S, Takayanagi K, Morooka S, Takabatake Y. QT prolongation and possibility of ventricular arrhythmias after intracoronary papaverine. *Cardiology* 1994; 84: 9–13.
  - 12 Barry DM, Xu H, Schuessler RB, Nerbonne JM. Functional knockout of the transient outward current, long-QT syndrome, and cardiac remodeling in mice expressing a dominant-negative Kv4 alpha subunit. *Cir Res* 1998; 83: 560–7.
  - 13 Jeron A, Mitchell GF, Zhou J, Murata M, London B, Buckett P, *et al*. Inducible polymorphic ventricular tachyarrhythmias in a transgenic mouse model with a long Q-T phenotype. *Am J Physiol* 2000; 278: H1891–8.
  - 14 Mitcheson JS, Chen J, Lin M, Culbertson C, Sanguinetti MC. A structural basis for drug-induced long QT syndrome. *Proc Natl Acad Sci USA* 2000; 97: 12 329–33.
  - 15 Sanguinetti MC, Jiang C, Curran ME, Keating MT. A mechanistic link between an inherited and an acquired cardiac arrhythmia: HERG encodes the  $I_{Kr}$  potassium channel. *Cell* 1995; 81: 299–307.
  - 16 Wang S, Liu S, Morales MJ, Strauss HC, Rasmusson RL. A quantitative analysis of the activation and inactivation kinetics of HERG expressed in *Xenopus* oocytes. *The J Physiol* 1997; 502 (Pt 1): 45–60.
  - 17 Rampe D, Murawsky MK, Grau J, Lewis EW. The antipsychotic agent sertindole is a high affinity antagonist of the human cardiac potassium channel HERG. *J Pharmacol Exp Ther* 1998; 286: 788–93.
  - 18 Redfern WS, Carlsson L, Davis AS, Lynch WG, MacKenzie I, Palethorpe S, *et al*. Relationships between preclinical cardiac electrophysiology, clinical QT interval prolongation and *torsade de pointes* for a broad range of drugs: evidence for a provisional safety margin in drug development. *Cardiovasc Res* 2003; 58: 32–45.
  - 19 Splawski I, Shen J, Timothy KW, Lehmann MH, Priori S, Robinson JL, *et al*. Spectrum of mutations in long-QT syndrome genes. KVLQT1, HERG, SCN5A, KCNE1, and KCNE2. *Circulation* 2000; 102: 1178–85.
  - 20 Suessbrich H, Schonherr R, Heinemann SH, Lang F, Busch AE. Specific block of cloned Herg channels by clofilium and its tertiary analog LY97241. *FEBS Lett* 1997; 414: 43–8.
  - 21 Li BX, Yang BF, Zhou J, Xu CQ, Li YR. Inhibitory effects of berberine on  $I_{K1}$ ,  $I_K$ , and HERG channels of cardiac myocytes. *Acta Pharmacol Sin* 2001; 22: 125–31.
  - 22 Kim CS, Son SJ, Kim HS, Kim YD, Lee KS, Jeon BH, *et al*. Modulating effect of ginseng saponins on heterologously expressed HERG currents in *Xenopus* oocytes. *Acta Pharmacol Sin* 2005; 26: 551–8.
  - 23 Kiehn J, Lacerda AE, Brown AM. Pathways of HERG inactivation. *Am J Physiol* 1999; 277: H199–210.
  - 24 Madeja M, Musshoff U, Speckmann EJ. Follicular tissues reduce drug effects on ion channels in oocytes of *Xenopus laevis*. *Eur J Neurosci* 1997; 9: 599–604.
  - 25 Choe H, Lee YK, Lee YT, Choe H, Ko SH, Joo CU, *et al*. Papaverine blocks hKv1.5 channel current and human atrial ultrarapid delayed rectifier  $K^+$  currents. *J Pharmacol Exp Ther* 2003; 304: 706–12.
  - 26 Mubagwa K, Shirayama T, Moreau M, Pappano AJ. Effects of PDE inhibitors and carbachol on the L-type Ca current in guinea pig ventricular myocytes. *Am J Physiol* 1993; 265: H1353–63.
  - 27 Zitron E, Karle CA, Wendt-Nordahl G, Kathofer S, Zhang W, Thomas D, *et al*. Bertosamil blocks HERG potassium channels in their open and inactivated states. *Br J Pharmacol* 2002; 137: 221–8.
  - 28 Milnes JT, Crociani O, Arcangeli A, Hancox JC, Witchel HJ. Blockade of HERG potassium currents by fluvoxamine: incomplete attenuation by S6 mutations at F656 or Y652. *Br J Pharmacol* 2003; 139: 887–98.
  - 29 Park JB, Choe H, Lee YK, Ha KC, Rhee KS, Ko JK, *et al*. Open channel block by KCB-328 [1-(2-amino-4-methanesulfonamidophenoxy)-2-[N-(3,4-dimethoxyphenethyl)-N-methylamino] ethane hydrochloride] of the heterologously expressed human ether-a-go-go-related gene  $K^+$  channels. *J Pharmacol Exp Ther* 2002; 302: 314–9.
  - 30 Snyders J, Knoth KM, Roberds SL, Tamkun MM. Time-, voltage-, and state-dependent block by quinidine of a cloned human cardiac potassium channel. *Mol Pharmacol* 1992; 41: 322–30.
  - 31 Smith PL, Baukrowitz T, Yellen G. The inward rectification mechanism of the HERG cardiac potassium channel. *Nature* 1996; 379: 833–6.
  - 32 Yang BF, Xu DH, Xu CQ, Li Z, Du ZM, Wang HZ, *et al*. Inactivation gating determines drug potency: a common mechanism for drug blockade of HERG channels. *Acta Pharmacol Sin* 2004; 25: 554–60.
  - 33 Walker BD, Valenzuela SM, Singleton CB, Tie H, Bursill JA, Wyse KR, *et al*. Inhibition of HERG channels stably expressed in a mammalian cell line by the antianginal agent perhexiline maleate. *Br J Pharmacol* 1999; 127: 243–51.
  - 34 Dun W, Jiang M, Tseng GN. Allosteric effects of mutations in the extracellular S5-P loop on the gating and ion permeation properties of the hERG potassium channel. *Pflugers Arch* 1999; 439: 141–9.
  - 35 Lees-Miller JP, Duan Y, Teng GQ, Duff HJ. Molecular determinant of high-affinity dofetilide binding to HERG1 expressed in *Xenopus* oocytes: involvement of S6 sites. *Mol Pharmacol* 2000; 57: 367–74.
  - 36 Webster R, Leishman D, Walker D. Towards a drug concentration effect relationship for QT prolongation and *torsades de pointes*. *Curr Opin Drug Discov Devel* 2002; 5: 116–26.
  - 37 Czarnecki W, Wielgus S. Effect of carriers and hydrophilic agents on papaverine spheres bioavailability. *Acta Pol Pharm* 1996; 53: 337–40.